Journal of Materials Chemistry A

Accepted Manuscript

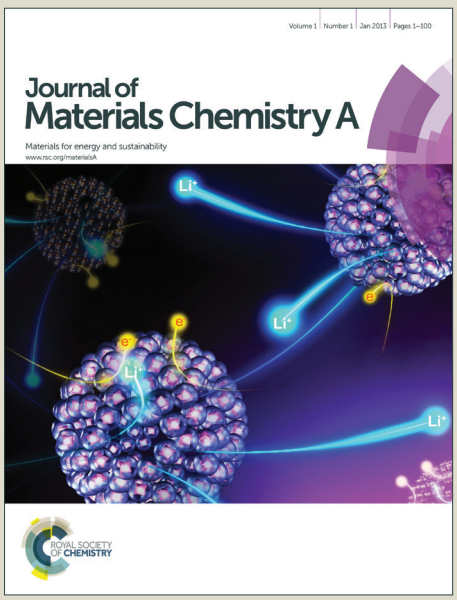

ROYAL SOCIETY OF CHEMISTRY

www.rsc.org/materialsA

Journal of Materials Chemistry A RSCPublishing

PAPER

Mesoporous Silica Nanoparticles for High Capacity Adsorptive Desulfurization

Cite this: DOI: 10.1039/x0xx00000x

Jessica M. Palomino,[a] Dat T. Tran[b,*] Jesse L. Hauser,[a] Hong Dong[c] and Scott R. J. Oliver[a,*]

Received 00th January 2012,
Accepted 00th January 2012

DOI: 10.1039/x0xx00000x

www.rsc.org/

Desulfurized JP-8 fuel is of great interest for use as the hydrogen feedstock of fuel cells. The refractory aromatic sulfur species present, however, are particularly challenging to remove through traditional methods. We report the first use of mesoporous silica nanoparticles (MSN) for desulfurization and the material displays a four-fold greater performance towards JP-8 fuel over previous sorbents. The bulk form of mesoporous silica shows three-fold greater level of desulfurization. Silver-impregnated nanoparticle and bulk MCM-41 were found to have saturation adsorption capacities of 32.6 mgS/g and 25.4 mgS/g, respectively. MSN display a high capacity for the notoriously difficult to remove 4,6-dimethyldibenzothiophene along with a two-fold improvement in breakthrough capacity over previously published materials, of 0.98 mgS/g at 10ppm$_w$S.

Introduction

Desulfurization of fossil fuels is vital for the environment and production of clean energy. Combustion of organosulfur-containing fuels results in the production of SO_x compounds, which cause health and environmental problems. These emissions have been linked to acid rain, climate change, and premature mortalities.[1, 2] In addition to their typical use in combustion engines, fossil fuels have also been utilized as hydrogen source for solid oxide fuel cells (SOFCs). SOFCs for both transport and non-transport energy are of interest to the military, especially for the auxiliary power of silent watch units.[3] JP-8 jet fuel is an ideal fuel source for such applications because it is highly abundant, hydrogen dense, and relatively safe to ship and store.[4] Unfortunately, the catalysts used in the fuel reformer and anode in the SOFC are gradually poisoned by the high concentration of sulfur compounds present in JP-8 (up to 3000 ppm$_w$S). For optimal use of JP-8 as a fuel source for SOFCs, a concentration of < 1 ppm$_w$S is desired though higher concentrations can still be used with reduced SOFC lifetime.[3, 5]

Hydrodesulfurization (HDS) is one of the most widely used forms of sulfur removal from fossil fuels and is successful in obtaining low ppm$_w$S ranges for lighter fuels such as gasoline. HDS is a high temperature, high pressure process that non-selectively hydrogenates. It lowers the octane level of fuel and requires hydrogen gas, giving the process a poor hydrogen economy. The HDS catalysts are also ineffective towards less reactive organosulfur compounds such as di- and tri-methylbenzothiophenes,[5-7] which are prevalent in JP-8 but less common in JP-5 and other lighter fuels.

To make SOFCs a reality for producing clean energy, a new method of desulfurization is needed that selectively removes organosulfur compounds. The method should be affordable, regenerable, portable, occur under ambient conditions, and require no additional hydrogen.[8] High surface area materials have been reported as potential desulfurization adsorbents and include activated carbon, mesoporous titania and silica, and zeolites loaded with one of a variety of metals including silver, copper, nickel, and zinc.[4, 7-10] While mesoporous silicas have been explored as desulfurization adsorbents, mesoporous silica nanoparticles (MSN) have remained largely unexplored. Recently, Fe_3O_4 magnetic core mesoporous silica microspheres were used to desulfurize model fuel, yielding capacities of 4.70 mgS/g after introducing $AgNO_3$.[11] MSNs are of interest for a variety of applications including drug delivery, catalysis, imaging, and sensing.[12-14] Their high surface area makes them a very promising framework for adsorptive desulfurization.

Most sorbents are tested on fuels lighter than JP-8, which are inherently easier to desulfurize. The difficulties of JP-8 desulfurization were highlighted by Tatarchuk and coworkers, who showed that silver-supported chromatographic silica displayed a maximum adsorption capacity for JP-8 of less than half that of JP-5.[15] A breakthrough capacity of ~ 1 mgS/g at 10 ppm$_w$S for JP-5 was reported. The sorbent was unable to bring JP-8 below 10 ppm$_w$S, which was attributed to its inability to remove the bulky di- and tri-methylbenzothiophenes that are prevalent in JP-8 but nearly absent in JP-5.[15]

A variety of silver-containing frameworks have been evaluated for desulfurization of fuels and model fuels, including the use of silver loaded bulk MCM-41 for JP-5.[16-18] High capacity adsorbents for use with JP-8, however, have yet to be realized. Here, we report an optimized approach utilizing mesoporous silica nanoparticles (MSN) as an improvement over bulk MCM-41 for adsorptive desulfurization of JP-8. The silver impregnated bulk mesoporous material (Ag-MCM-41)

and MSN (Ag-MSN) display adsorption capacities of 24.5 mgS/g and 32.6mgS/g, respectively.

Experimental

Materials
All chemicals were used as received without further purification. Tetraethylorthosilicate (TEOS), benzothiophene (BT), and dibenzothiophene (DBT) were all obtained from Acros Organics. Sodium hydroxide and naphthalene (NA) were obtained from Fisher Scientific. Cetyltrimethylammonium bromide (CTAB), diethyl ether, and bulk MCM-41 were obtained from Sigma Aldrich. Silver nitrate was obtained through MP Biomedicals, decane from TCI and 4,6-dimethyldibenzothiophene (DMDBT) from Frontier Scientific.

Preparation of MSN
MCM-41 nanoparticles (MSN) were synthesized using a method we previously published.[19] A solution containing 1.0 g CTAB, 0.28 g NaOH, and 483.5 g doubly distilled deionized water was stirred at 80 ^{o}C at a rate of 625 rpm. After a minimum of 15 minutes, 4.58 g TEOS was added dropwise over a two minute period. Stirring was continued for an additional 2 hours, followed by 30 minutes of static aging at room temperature prior to filtering and rinsing with copious amount of doubly distilled deionized water. The product was then dried, ground, and calcined at 560 ^{o}C for 4 hours with an initial ramp rate of 1 ^{o}C/min.

Preparation of Ag-MCM-41 and Ag-MSN
MCM-41 and MSN were loaded with the desired amount of silver *via* wet impregnation. Silver nitrate was dissolved in a water/ethanol solution and added dropwise to the frameworks. Once the samples were wet, they were placed in a 110 ºC vacuum oven to dry. These steps were repeated until the sample had adsorbed all the silver from solution. To achieve 18 wt.% and 20 wt.% Ag, 0.283 g and 0.315 g of $AgNO_3$, respectively, were used per gram of framework material.

Characterization of MCM-41 and MSN
Powder X-ray Diffraction (PXRD) was performed on a Rigaku SmartLab X-ray diffractometer with Cu Kα radiation. Samples were analyzed from 2º to 80º (2θ) with a step size of 0.01º. BET surface area of the samples was measured by physical adsorption of N_2 at 77 K using a Micromeritics physisorption analyzer (TriStar II 3020 v1.03). Adsorption/desorption isotherm measurements were collected in the relative pressure range (P/P_o) from 0.01 to 1.00. Scanning electron microscopy (SEM) and scanning transmission electron microscopy (STEM) data were collected with a FEI Quanta 3D Dualbeam microscope. Transmission electron microscopy (TEM) was collected using a JEOL 2100F microscope operated at 200 kV. Samples were prepared for TEM by sonication in acetone for 3 minutes prior to dispersal on a TEM grid covered in holey carbon film.

JP-8 and model fuel testing
Prior to all JP-8 and model fuel testing, the adsorbents were heated under vacuum at 110 °C overnight to remove trapped gas or water. All model fuel tests were performed using 500 ppm_wS fuel in decane (equivalent molarity with NA for selectivity studies). Silver optimization was performed with DBT as the model fuel contaminant. Additional model fuel data were obtained using DMDBT, BT, and NA as contaminants. All model fuel tests were done with a 50:1 model fuel to sorbent weight ratio with a 1 hour batch soak time. For column tests (breakthrough and regeneration), the prepared materials were packed in a Chromtech column (4.6 mm ID, 50 mm length). JP-8 fuel containing an initial sulfur concentration of ~ 517 ppm_wS was pumped at 0.5 mL/min into the column using a Shimadzu HPLC pump. Column and 24 hour batch (beaker) test experiments were analyzed for total sulfur concentration using a UV total sulfur analyzer (multi EA 3100, Analytikjena) with a detection limit of 45 ppb. Typical batch test experiments were performed with ~ 0.05 g of sorbent in ~ 5.5 g of JP-8, whereas column experiments used ~ 0.18 g of sorbent and up to 40 mL of JP-8 (or until the sorbent was saturated). Regeneration was achieved by running between 50 and 60 mL of diethyl ether through the column and drying in a 110 °C vacuum oven before further analysis. Infrared spectra were recorded using a Perkin-Elmer Spectrum-One FT-IR where samples were dried at 110 °C under vacuum before forming KBr pellets. Inductively Coupled Plasma (ICP) was collected on a Perkin-Elmer Optima 7000 DV.

Results and Discussion

Physical properties of the sorbents
Commercially available pure silica MCM-41 and MSN were loaded with an optimized amount of Ag *via* wet impregnation to form Ag-MCM-41 and Ag-MSN, respectively. The structure of both unloaded and silver loaded MCM-41 (Figure S1) and MSN (Figure 1) was confirmed by PXRD. The (100), (110), (200), and (210) reflections are observed in both unloaded and silver loaded samples, confirming that the impregnation procedure does not compromise the overall framework integrity. Neither metallic silver nor $AgNO_3$ peaks are observed (Figure 1, inset), suggesting that the silver is well dispersed. BET analysis shows that while the majority of surface area for both frameworks is retained after Ag loading, Ag-MSN has significantly higher surface area than Ag-MCM-41, as expected (Table 1, isotherms Figure S2 to S5). A similar

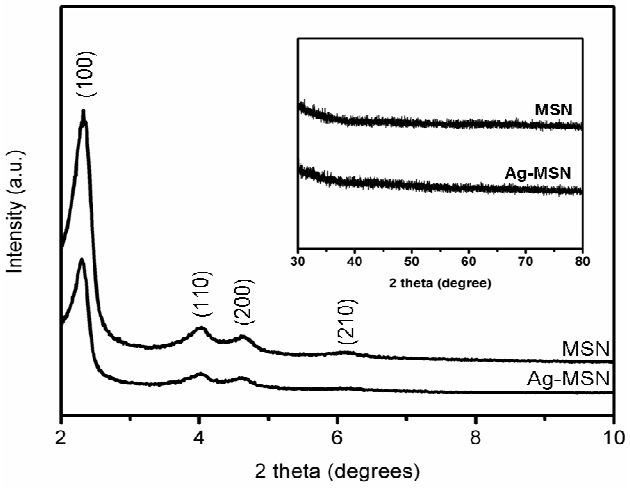

Fig. 1. PXRD of loaded and unloaded MSN with characteristic MCM-41 reflections labeled. Inset: the lack of higher angle peaks indicates that the silver is well dispersed.

decrease is also seen in the BJH pore volume before and after silver loading for both sorbents. The pore diameters remain relatively constant before and after loading.

Table 1. Structural properties obtained from N_2 adsorption/desorption data.

Sorbent	BET Surface Area (m^2/g)	BJH Pore Volume (cm^3/g)[a]	BJH Pore Diameter (nm)[b]
MCM-41	883.6	1.05	3.0
Ag-MCM-41	528.4	0.61	3.1
MSN	1067.8	1.35	2.9
Ag-MSN	702.5	0.93	3.0

[a]BJH adsorption pore volume; [b]BJH adsorption average pore diameter

The UV-Visible diffuse reflectance spectrum of Ag-MSN shows a high intensity peak around 250 nm (Figure 2). This peak is indicative of Ag^+, commonly seen in silver-loaded MCM-41.[20, 21] A smaller band at ~ 310 nm likely indicates the presence of $Ag_n^{\delta+}$. A small silver oxide content is typically expected based on the neutral charge of the silica framework.[20, 21] Ag-MSN lacks any peak at 400 nm that would indicate the presence of metallic silver,[20, 21] in agreement with the PXRD data. The UV-Vis diffuse reflectance spectra for Ag-MCM-41 shows the same peaks as Ag-MSN (Figure S6).

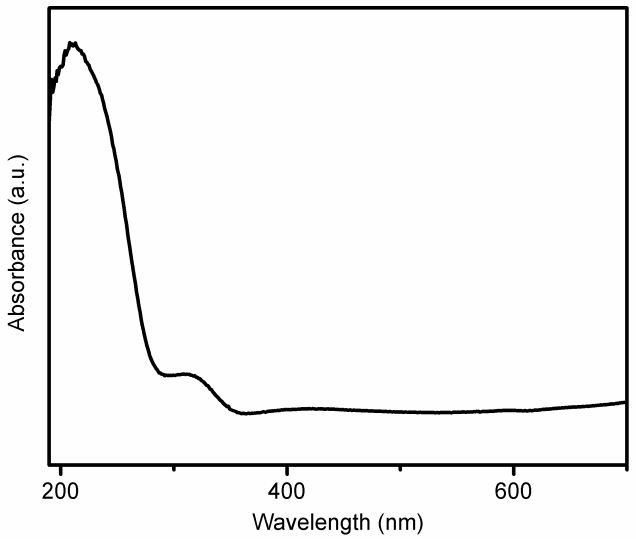

Fig. 2. UV-Vis diffuse reflectance spectrum of Ag-MSN.

As expected, STEM and SEM analyses (Figures 3 and 4) reveal the starkly different morphologies between the MSN and MCM-41. MSN consists of spherical nanoparticles with an average diameter of approximately 80 nm, while the MCM-41 contains a variety of particle shapes in the micron range. MSN (Figure 5) and Ag-MSN (Figure 6) were further analyzed by TEM. Once the sample is impregnated with silver, TEM (Figure 6) shows that the silver is uniformly dispersed across the nanoparticle. Small clusters are present throughout the nanoparticle, the largest approximately 5 nm in diameter with the majority of the visible clusters less than 2 nm.

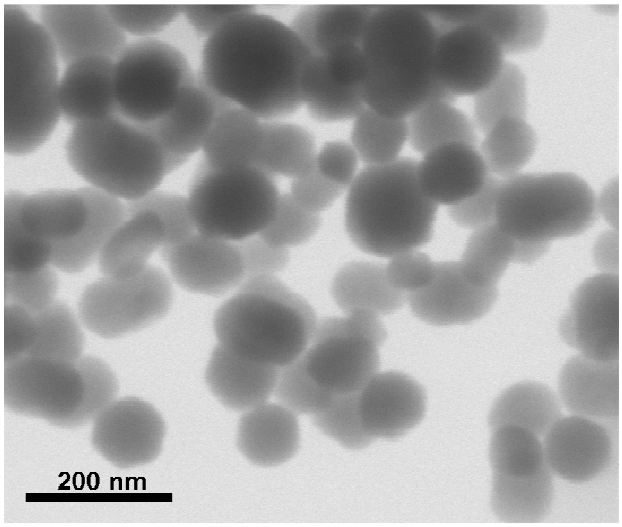

Fig. 3. STEM micrograph of MSN.

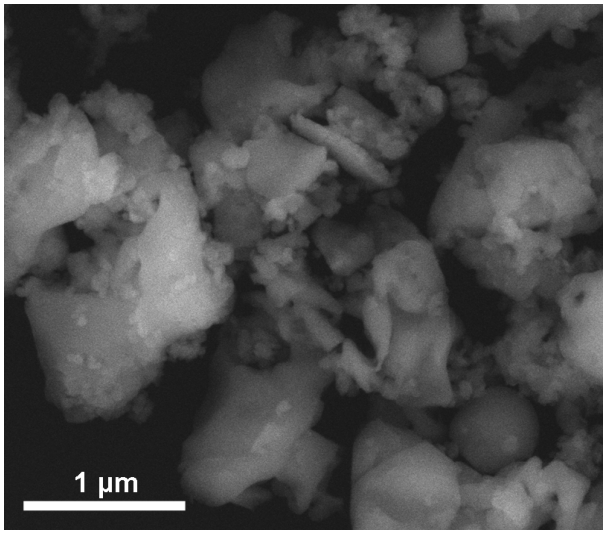

Fig. 4. SEM micrograph of MCM-41.

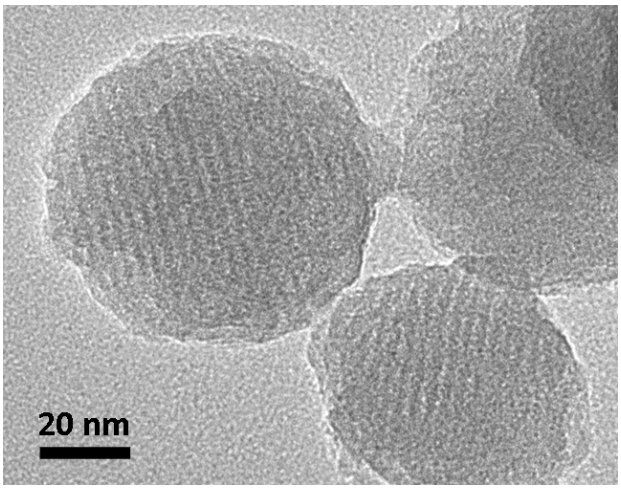

Fig. 5. TEM micrograph of MSN.

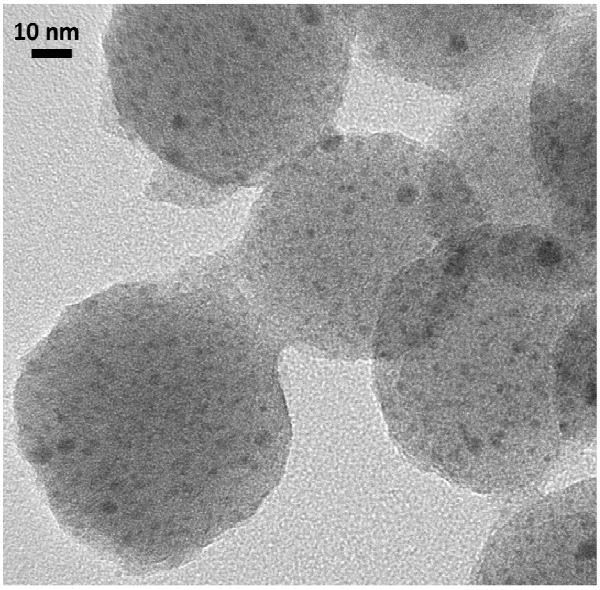

Fig. 6. TEM micrograph of Ag-MSN.

JP-8 fuel tests and regeneration

The silver optimization for MSN is shown in Figure 5 using model fuel. The adsorption capacity increases with the silver loading until a maximum adsorption capacity of 12.7 mgS/g for 20 wt.% Ag loading (Figure 7). The maximum adsorption capacity decreased to 9.4 mgS/g when silver was further increased to 25 wt.%. This decrease in capacity may be a result of silver or silver nitrate aggregates forming in the channels and blocking adsorption sites. A similar phenomenon is observed with silver loaded TiO_2, where increased silver loading decreases surface area and pore volume due to the formation of silver agglomerates.[15] Based on this optimization, 20 wt.% was used for all subsequent studies of Ag-MSN. 18 wt.% was found to be optimal for Ag-MCM-41 by a similar optimization procedure (Figure S7).

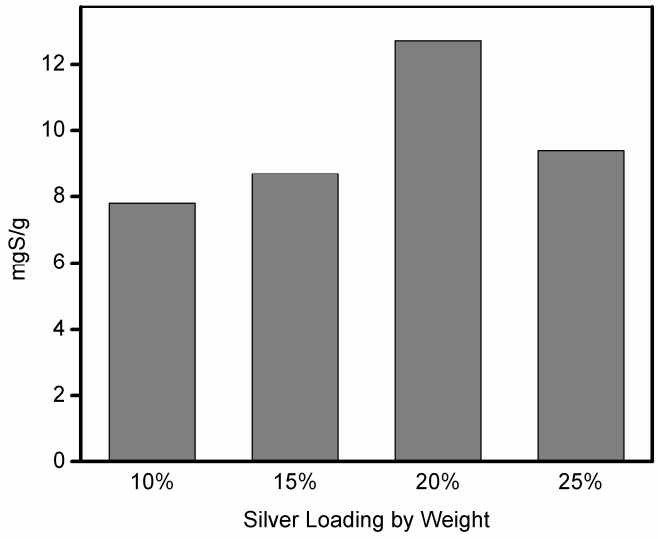

Fig. 7. Optimization of silver loading for MSN using 500 ppm_wS model fuel of DBT in decane.

Sulfur adsorption capacities were measured using JP-8 fuel at room temperature over a 24 hour period (Table 2). Ag-MSN was found to have a four-fold increase in capacity, 32.6 mgS/g, compared to other sorbents published for JP-8.[22-24]

Table 2. 24-hour adsorption capacities using JP-8 for MCM-41 and MSN pre- and post-loading with optimized amount of silver and the highest previously published values.[22]

Sorbent	Optimized Adsorption Capacity (mgS/g)	Silver Efficiency (mol S/mol Ag)
Unloaded MCM-41	0.8	-
Ag-MCM-41	25.4	0.48
Unloaded MSN	4.6	-
Ag-MSN	32.6	0.55
Ag-TiO_x-Al_2O_3[22]	8.01	0.27

A recent publication by Tatarchuck and coworkers reported a silver loaded TiO_x-Al_2O_3 material with a maximum adsorption capacity of 8.01 mgS/g for JP-8, surpassing the previously reported values of 5.7 mgS/g for silica-supported gold and 6.11 mgS/g of silver loaded TiO_x-Al_2O_3.[22, 24] Table 2 also highlights the increased efficiency of both Ag-MSN and Ag-MCM-41 with respect to both overall capacity and uptake normalized to silver loading. While both are loaded with an optimized amount of silver, a greater fraction of the silver sites are utilized for adsorption in Ag-MSN, likely because of its greater specific surface area. Packed column experiments for Ag-MSN and Ag-MCM-41 at room temperature again show the superior capacity of Ag-MSN to Ag-MCM-41 (Figure 8). Both materials yield an initial eluent concentration of 0 ppm_wS, underscoring the strong ability of our materials to adsorb the notoriously difficult trimethyldibenzothiophene species. Breakthrough capacities at 10 ppm_wS are 0.98 mgS/g and 0.21 mgS/g for Ag-MSN and Ag-MCM-41, respectively. This compares favorably with the previously reported 0.38 mgS/g at 10ppm_wS for JP-8.[22] Other published materials have been unable to obtain sub 10 ppm_wS levels due their inability to remove the di- and tri-methylated dibenzothiophenes found in JP-8.[22]

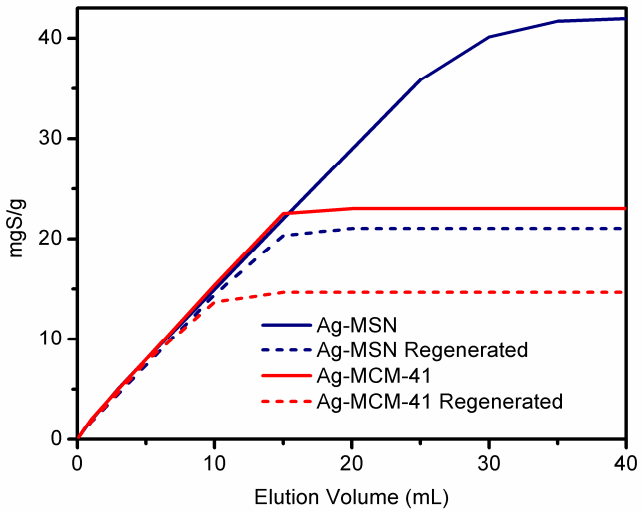

Fig. 8. Column and regeneration studies of Ag-MCM-41 and Ag-MSN with JP-8.

The materials were solvent regenerated using diethyl ether. Batch model fuel testing yields an adsorption capacity of 9.2 mgS/g for Ag-MSN after solvent regeneration, corresponding to ~ 70% retention, which is substantially higher than 50% which has been previously reported using thermal regeneration.[17] ICP analysis shows the silver content of Ag-MSN decreases by 30% after regeneration, which explains the decrease in adsorption capacity. In column studies, only 50% of the total adsorption capacity is maintained after the first regeneration. Because of this drop in capacity between the first and second cycle, further regeneration was not studied for this initial report. FT-IR data confirms that dibenzothiophene is completely removed from the framework after solvent regeneration with diethyl ether (Figure 9).

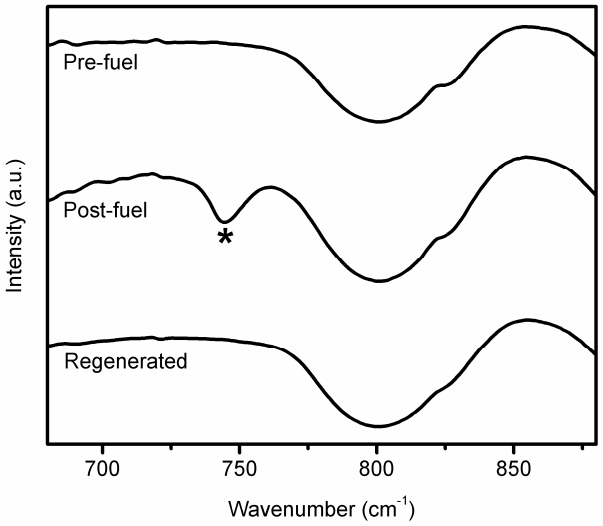

Fig. 9. FT-IR of Ag-MSN prior to fuel exposure (top), after 1 hr in 500 ppm_wS model fuel of dibenzothiophene in decane (middle), and after solvent regeneration using diethyl ether (bottom). The stretch from DBT is denoted with an asterisk.

Binding studies and model fuel comparison

Previous literature proposes two potential mechanisms of adsorption of sulfur aromatics towards silver loaded sorbents: direct S-M binding or a selective π-complexation. To further resolve the adsorption mechanism, we performed an FT-IR study and observed a dibenzothiophene peak shift from 734 cm^{-1} (unbound) to 743 cm^{-1} (adsorbed onto Ag-MSN). This result indicates that the dibenzothiophene binds in a perpendicular fashion with respect to the adsorbent surface.[25] This orientation of the dibenzothiophene molecule therefore supports a S-M binding mechanism.

Comparison studies using different model fuels can reveal insight into the binding mechanism between framework and contaminant.[26-28] Ag-MSN was exposed to four different model fuels in isomolar concentration equivalent to 500 ppm_wS (for those containing sulfur), and the one hour adsorption capacities are shown in Figure 10. Dibenzothiophene and DMDBT have larger adsorption capacities than benzothiophene, which correlates to the higher electron density on their sulfur atom as calculated using density functional theory.[26] Furthermore, the sterically hindered sulfur on DMDBT leads to a lower adsorption capacity, pointing to direct S-M binding as a likely adsorption mechanism. The sulfur-free naphthalene was still adsorbed by Ag-MSN, demonstrating that π-complexation must also be occurring.

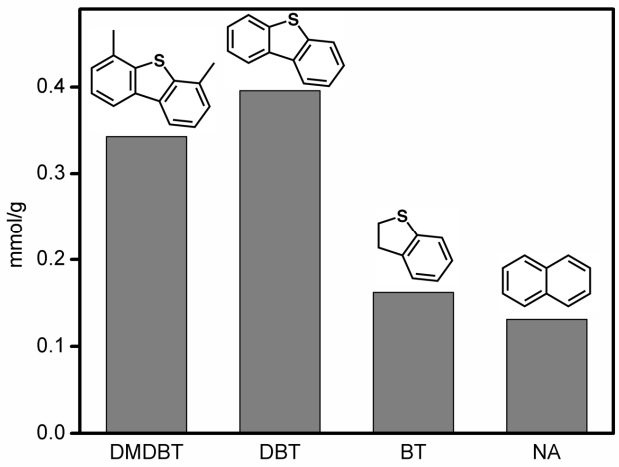

Fig. 10. 1 hour adsorption capacities for Ag-MSN in single contaminant model fuels. 4,6-dibenzothiophene (DMDBT), dibenzothiophene (DBT), and benzothiophene (BT) are all 500 ppm_wS and naphthalene (NA) is isomolar to them.

Conclusions

In summary, Ag-MSN is a highly effective adsorbent for JP-8 desulfurization, one of the most challenging fuels to desulfurize. The mesoporous nanoparticle host displays an adsorption capacity of 32.6 mgS/g, which is significantly greater than previously published materials. The high capacity towards dimethylated dibenzothiophene, record breakthrough capacity at 10 ppm_wS for JP-8 and regenerability of ~ 70% underscore its potential as an effective desulfurization adsorbent. Currently, our lab is researching methods such as anchoring to increase the regenerability of this material, particularly for improving its regeneration performance in column studies. The optimization of the silver content within the mesoporous structure and solvent regeneration capability demonstrate a distinct advantage over previously reported materials.[17] FT-IR measurements and model fuel tests support an S-M binding as the major mode of adsorption, while π-complexation likely also plays a role. The higher surface area and smaller particle size likely contributes to the better performance of MSN over bulk MCM-41. Our material represents a significant step to reducing sulfur content to a level that may allow the use of JP-8 as the hydrogen source for SOFCs.

Acknowledgements

This work was supported by DOD ARL, Contract No. W911NF-12-2-0005. The PXRD data in this work were recorded on an instrument supported by the NSF Major Research Instrumentation (MRI) Program under Grant DMR-1126845. We acknowledge Dr. Tom Yuzvinsky for image acquisition and the W.M. Keck Center for Nanoscale Optofluidics at UC Santa Cruz for use of the FEI Quanta 3D Dualbeam microscope. ICP experiment assistance from Rob

Franks in the Department of Earth and Marine Sciences at UC Santa Cruz is also acknowledged.

Notes and references

[a] Department of Chemistry and Biochemistry, University of California, Santa Cruz, California 95064, USA. Fax: 831-459-2935; Tel: 831-459-5448; E-mail: soliver@ucsc.edu

[b] U.S. Army Research Laboratory, RDRL-SED-C, 2800 Powder Mill Road, Adelphi, Maryland 20783-1138, USA. Fax: 301-394-0273; Tel:301-394-0293; E-mail: dat.t.tran4.civ@mail.mil

[c] U.S. Army Research Laboratory, Aberdeen Proving Ground, Maryland 21005, USA.

† Electronic Supplementary Information (ESI) available: Additional characterization data. See DOI: 10.1039/b000000x/

1. S. R. H. Barrett, R. E. Britter and I. A. Waitz, *Environmental Science & Technology*, 2010, **44**, 7736-7742.
2. S. R. H. Barrett, S. H. L. Yim, C. K. Gilmore, L. T. Murray, S. R. Kuhn, A. P. K. Tai, R. M. Yantosca, D. W. Byun, F. Ngan, X. Li, J. I. Levy, A. Ashok, J. Koo, H. M. Wong, O. Dessens, S. Balasubramanian, G. G. Fleming, M. N. Pearlson, C. Wollersheim, R. Malina, S. Arunachalam, F. S. Binkowski, E. M. Leibensperger, D. J. Jacob, J. I. Hileman and I. A. Waitz, *Environmental Science & Technology*, 2012, **46**, 4275-4282.
3. A. Samokhvalov and B. J. Tatarchuk, *Catalysis Reviews*, 2010, **52**, 381-410.
4. A. J. Hernández-Maldonado and R. T. Yang, *Catalysis Reviews*, 2004, **46**, 111-150.
5. R. T. Yang, A. J. Hernández-Maldonado and F. H. Yang, *Science*, 2003, **301**, 79-81.
6. C. Song, *Catalysis Today*, 2003, **86**, 211-263.
7. X. Ma, L. Sun and C. Song, *Catalysis Today*, 2002, **77**, 107-116.
8. S. Velu, X. Ma, C. Song, M. Namazian, S. Sethuraman and G. Venkataraman, *Energy & Fuels*, 2005, **19**, 1116-1125.
9. J. H. Kim, X. Ma, A. Zhou and C. Song, *Catalysis Today*, 2006, **111**, 74-83.
10. A. H. M. Shahadat Hussain and B. J. Tatarchuk, *Fuel*, 2013, **107**, 465-473.
11. P. Tan, J.-X. Qin, X.-Q. Liu, X.-Q. Yin and L.-B. Sun, *Journal of Materials Chemistry A*, 2014, **2**, 4698-4705.
12. I. I. Slowing, J. L. Vivero-Escoto, C.-W. Wu and V. S. Y. Lin, *Advanced Drug Delivery Reviews*, 2008, **60**, 1278-1288.
13. I. I. Slowing, B. G. Trewyn, S. Giri and V. S. Y. Lin, *Advanced Functional Materials*, 2007, **17**, 1225-1236.
14. C.-H. Lee, S.-H. Cheng, Y.-J. Wang, Y.-C. Chen, N.-T. Chen, J. Souris, C.-T. Chen, C.-Y. Mou, C.-S. Yang and L.-W. Lo, *Advanced Functional Materials*, 2009, **19**, 215-222.
15. S. Nair and B. J. Tatarchuk, *Fuel*, 2010, **89**, 3218-3225.
16. S. G. McKinley and R. J. Angelici, *Chemical Communications*, 2003, 2620-2621.
17. H. Chen, Y. Wang, F. H. Yang and R. T. Yang, *Chemical Engineering Science*, 2009, **64**, 5240-5246.
18. A. J. Hernández-Maldonado and R. T. Yang, *Industrial & Engineering Chemistry Research*, 2002, **42**, 123-129.
19. M. A. Gonzales, H. Han, A. Moyes, A. Radinos, A. J. Hobbs, N. Coombs, S. R. J. Oliver and P. K. Mascharak, *Journal of Materials Chemistry B*, 2014, **2**, 2107-2113.
20. S. Sohrabnezhad and A. Pourahmad, *Spectrochimica Acta Part A: Molecular and Biomolecular Spectroscopy*, 2012, **86**, 271-275.
21. A. Yin, C. Wen, W.-L. Dai and K. Fan, *Applied Catalysis B: Environmental*, 2011, **108-109**, 90-99.
22. A. H. M. S. Hussain, H. Yang and B. J. Tatarchuk, *Energy & Fuels*, 2013, **27**, 4353-4362.
23. A. H. M. Shahadat Hussain and B. J. Tatarchuk, *Fuel*, 2012.
24. D. T. Tran, Z. W. Dunbar and D. Chu, *International Journal of Hydrogen Energy*, 2012, **37**, 10430-10434.
25. H. Shang, C. Liu and F. Wei, *Journal of Natural Gas Chemistry*, 2004, **13**, 95-100.
26. T. Ke and H. Xin, *Petroleum Science and Technology*, 2010, **28**, 573-581.
27. H. Lu, C. Deng, W. Ren and X. Yang, *Fuel Processing Technology*, 2014, **119**, 87-91.
28. J. Bu, G. Loh, C. G. Gwie, S. Dewiyanti, M. Tasrif and A. Borgna, *Chemical Engineering Journal*, 2011, **166**, 207-217.

Table of Contents Entry

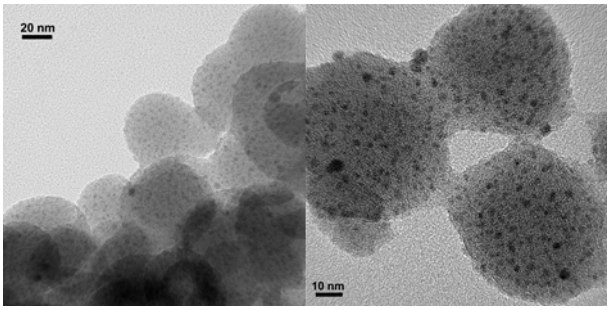

Silver-loaded mesoporous silica nanoparticles were applied for the first time to the desulfurization of JP-8 fuel with record breaking performance.